UDC: 617.53-002.191-006.2-036.1-07-089 http://dx.doi.org/10.23999/j.dtomp.2017.1.3

Journal of Diagnostics and Treatment of Oral and Maxillofacial Pathology

Free online article at www.dtjournal.org

omf publishing

Features of Diagnostics, Clinical Course and Treatment of the Branchial Cleft Cysts

Oleksii O. Tymofieiev[1,*], Ievgen I. Fesenko[2], Olga S. Cherniak[3], Valentyna I. Zaritska[4]

[1] Chair of the Department of Maxillofacial Surgery, Stomatology Institute, Shupyk National Medical Academy of Postgraduate Education, Kyiv, Ukraine *(ScD, Prof)*
[2] Oral and Maxillofacial Surgery Department, KMU of UAFM, Kyiv, Ukraine *(Assis Prof)*
[3] Head of the Department of Ultrasound at the Regional Diagnostic Center, Kyiv Regional Clinical Hospital, Kyiv, Ukraine
[4] Department of Pathology, Shupyk National Medical Academy of Postgraduate Education, Kyiv, Ukraine *(PhD, Assoc Prof)*

ABOUT ARTICLE

Article history:
Paper received 03 October 2016
Accepted 08 November 2016
Available online 18 February 2017

Keywords:
Branchial cleft cysts (BCCs)
Branchiogenic carcinoma
Ultrasound
Echogenicity
Color Doppler Ultrasound
Power Doppler Ultrasound
Pseudosolid appearance

ABSTRACT

Purpose.
The aim of the present study was to determine the features of diagnostics, clinical course and treatment of the branchial cleft cysts.
Patients and methods.
The study composed of the branchial cleft cysts investigation and their complications in patients of different age groups, methods of diagnostics, anatomical features, surgical stages and pathomorphological study.
Results.
Diagnostic value of sonography, MDCT and MRI, pathomorphological study in verification of branchial cleft cysts and their complications have been proved. Surgical treatment technique is presented.
Conclusion.
Presented methods of diagnostics of the branchial cleft cysts and their complications, variants of clinical course and treatment can reduce the risk of failure at the pre-, intra- and post-operative stages.

Introduction

Branchial cleft cyst (*synonyms:* lateral cyst of the neck, congenital lateral cyst of the neck, branchial cyst, lateral branchial cyst of the neck, lateral lymphoepithelial cyst) according to our data has been found in 25% of all cysts of the soft tissue in maxillofacial and neck area [1-15]. The branchial cleft fistulas are rarely detected.

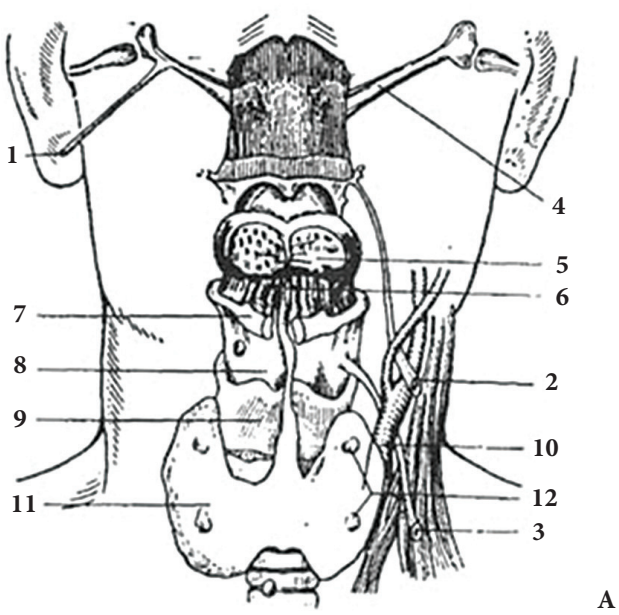

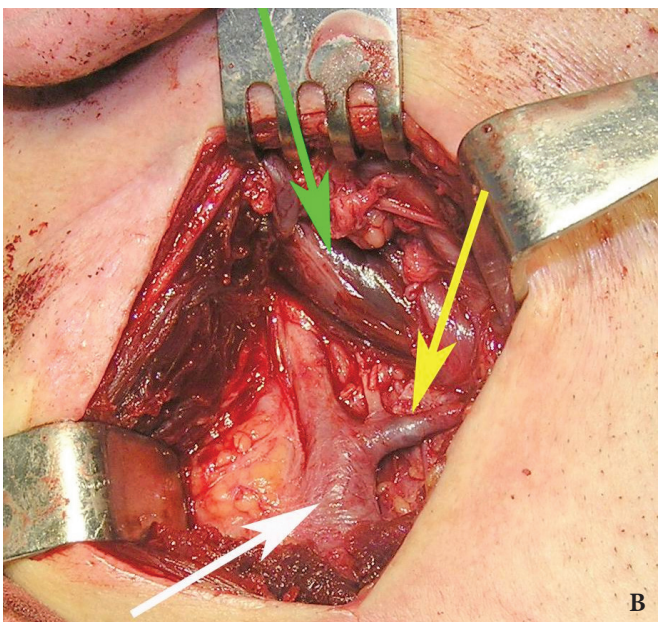

FIGURE 1. Location scheme of branchial neck fistulas (**A**): 1 – I branchial pocket; 2 – II branchial pocket; 3 – III branchial pocket; 4 – auditory tube; 5 – tongue; 6 – thyroglossal duct; 7 – the hyoid bone; 8 – thyroid-hyoid membrane; 9 – thyroid cartilage; 10 – common carotid artery; 11 – thyroid gland; 12 – parathyroid glands. Location of the inner pole (**B**) of BCC after its removal. Internal jugular vein is marked by *white arrow*, facial vein – *yellow arrow*, posterior belly of the digastric muscle – *green arrow*.

* *Corresponding author. Department of Maxillofacial Surgery, Stomatology Institute, Shupyk NMAPE, 4-a Pidvysotskogo Street, Kyiv 01103, Ukraine. Tel., fax: +38 (044) 528 35 17. E-mail address: tymofeev@gmail.com (O.O. Tymofieiev)*

Branchial cleft cysts (Greek, *branchia* gill) have dysontogenetic origin.

With regard to the pathogenesis of branchial cleft cysts (BCCs) and fistulas there is disagreement till present day. There are two theories of its origin. According to the **"thymus"** theory these cysts and fistulas are formed from the remnants of thymopharyngeal duct. **"Branchial"** theory links the origin of these lesions with abnormal development of branchial (pharyngeal) pockets. Anomalies of the 2nd or 3rd pair of pharyngeal (branchial) pockets are the source of the formation of the BCCs and fistulas. Internal branchial pockets are formed by endoderm and the external (or grooves) by ectodermal germ layers. BCCs can be both of endodermal and ectodermal origin (Fig 1A).

Cysts occur at any age, but are much more common in children and young adults (Fig 2). Their appearance is preceded (provoke) by the infections of the respiratory tracts (tonsillitis, flu, etc.). The sizes of the BCCs can be different (Fig 2). In contrary to dermoid (epidermoid) cysts the BCCs are often suppurate [1, 2, 3].

First, BCCs were classified according to their localization. Bailey H. (1929), divided them into 4 types [16]: **type 1** – deep to platysma, anterior to sternocleidomastoid (SCM); **type 2** – abutting internal carotid artery and adherent to internal jugular vein (most common); **type 3** – extending between internal and

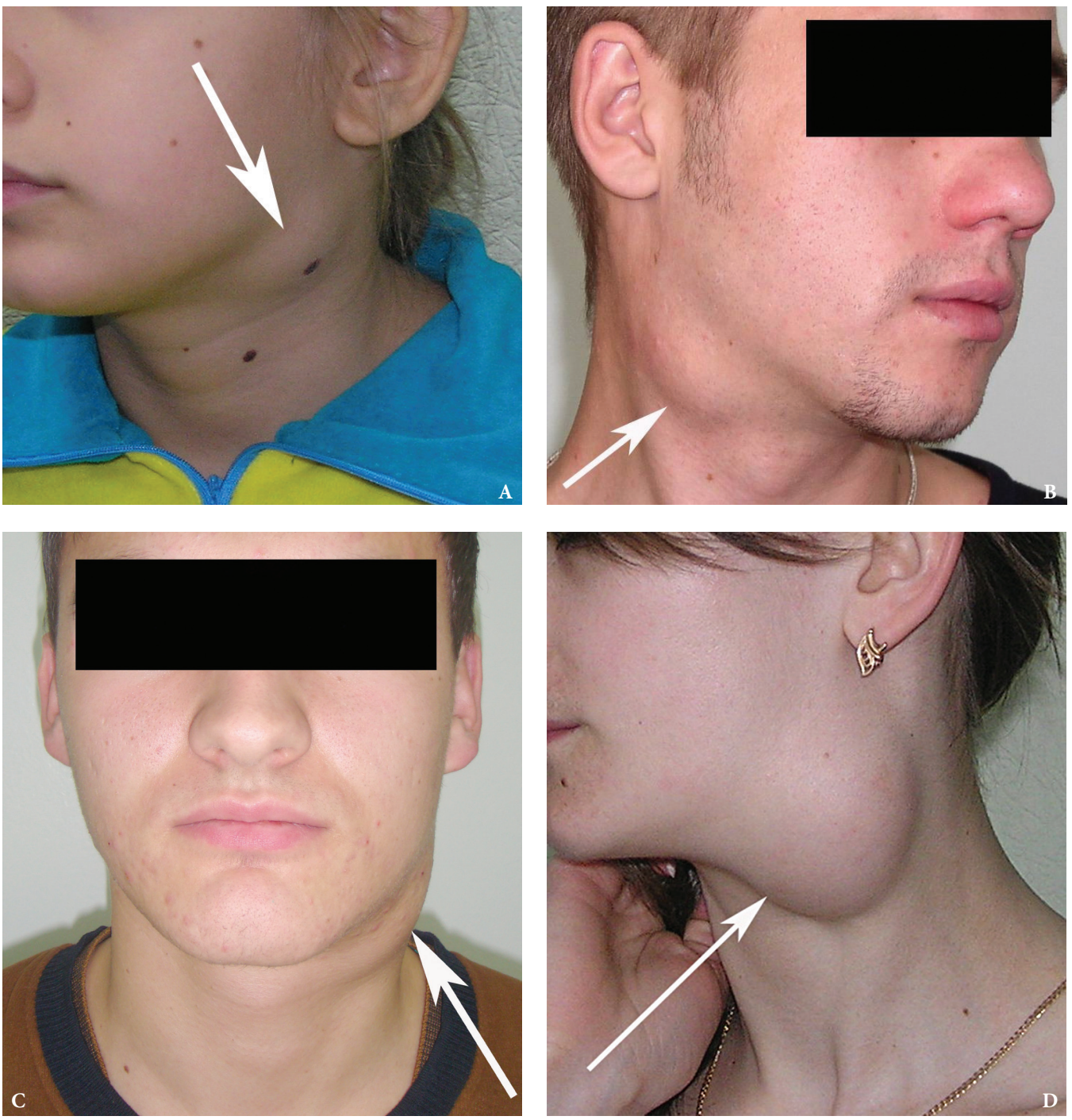

FIGURE 2. Clinical view of the patients of different ages with BCCs (*arrows*) of various sizes (**A**, **B**, **C**, **D**). **(Fig 2 continued on the next page.)**

external carotid arteries; **type 4** – abutting pharyngeal wall and potentially extending superiorly to skull base.

CLINICAL PICTURE

BCCs are the round-shaped mass at the upper neck anteriorly to the sternocleidomastoid muscle (in carotid triangle). At the same time, they may be located in the middle and even lower parts of the neck. Typically, the BCCs localized in the upper or middle third of the neck adjacent to the anterior edge of the sternocleidomastoid muscle or partly comes under it. It is located between the 2nd and 3rd fascial leaf of the neck (between the superficial and deep fascia leaf of the own neck fascia) on the neurovascular bundle. The upper pole of the cyst is often found near or under the posterior edge of the digastric or stylohyoid muscles. Medially the cysts are adjacent to the internal jugular vein at the level of common carotid artery bifurcation. BCCs can be located in the upper, middle and lower parts of the neck. Along the length the cyst may extend down to the clavicle, and in the upper part of the neck reaches mastoid process (Fig 1B).

Visually, BCCs are showning as a painless limited rounded shape tumor-like lesion with a smooth surface. The skin above it is not changed in color. They are not soldered with surrounding tissues. A compulsory component of the

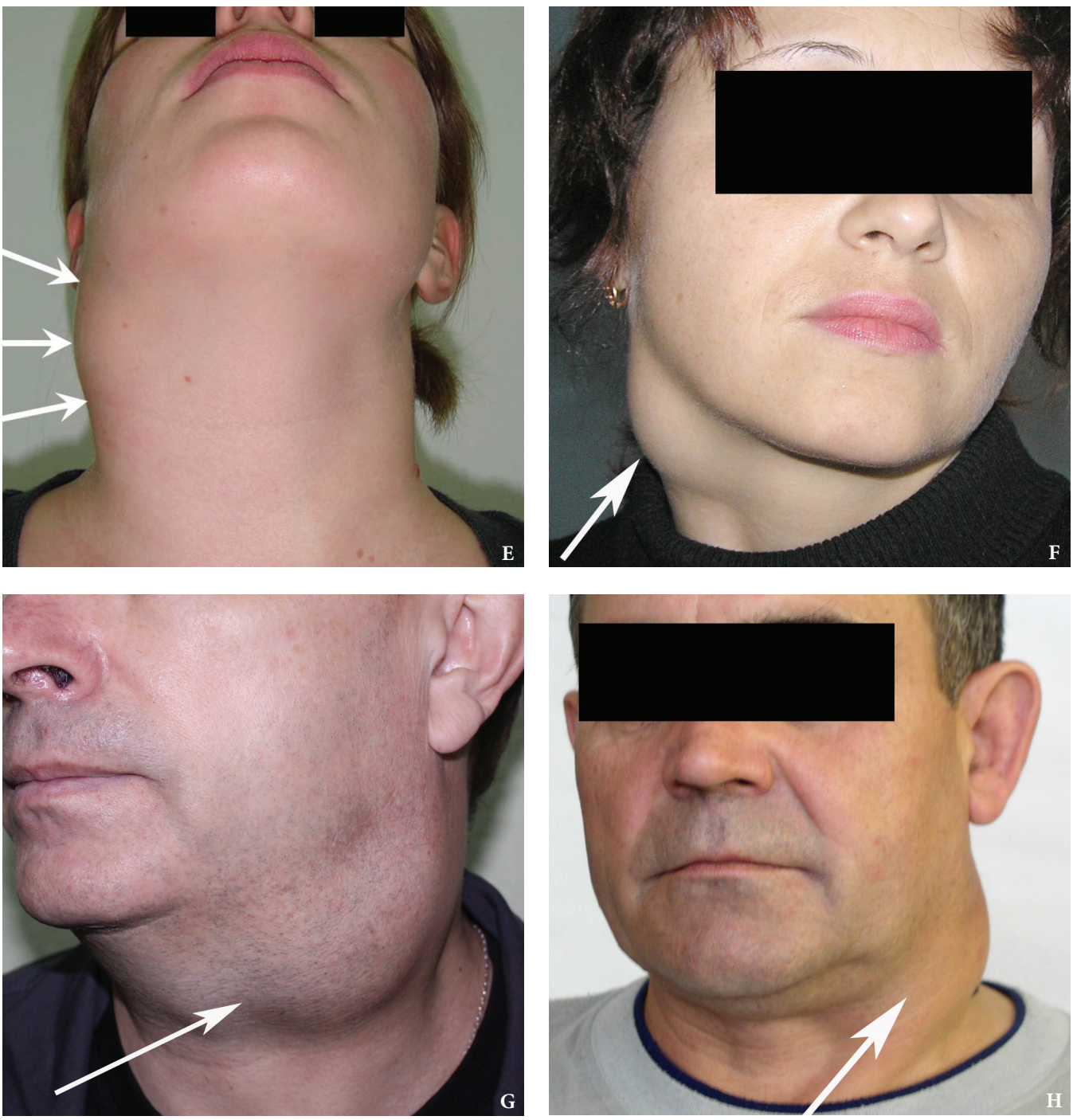

FIGURE 2 (cont'd). Clinical view of the patients of different ages with BCCs (*arrows*) of various sizes (**E**, **F**, **G**, **H**). **(Fig 2 continued on the next page.)**

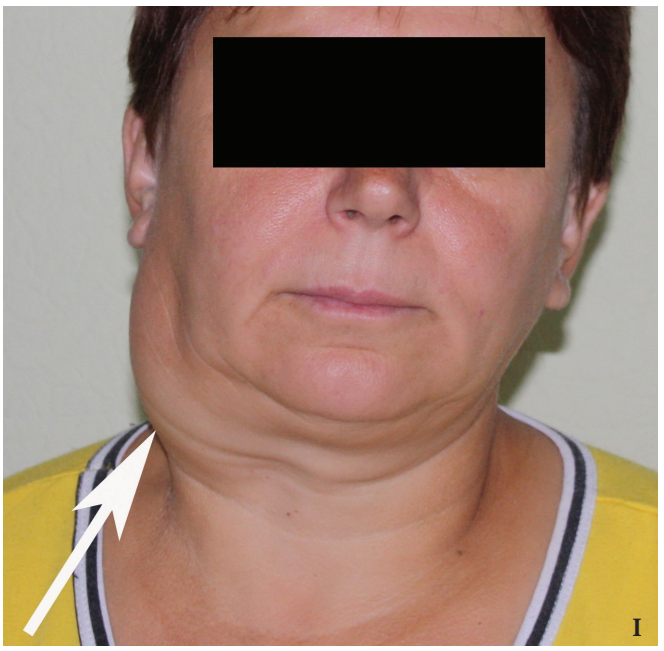

FIGURE 2. (**cont'd**) Clinical view of female with the non-infected BCC (*arrow*) (**I**).

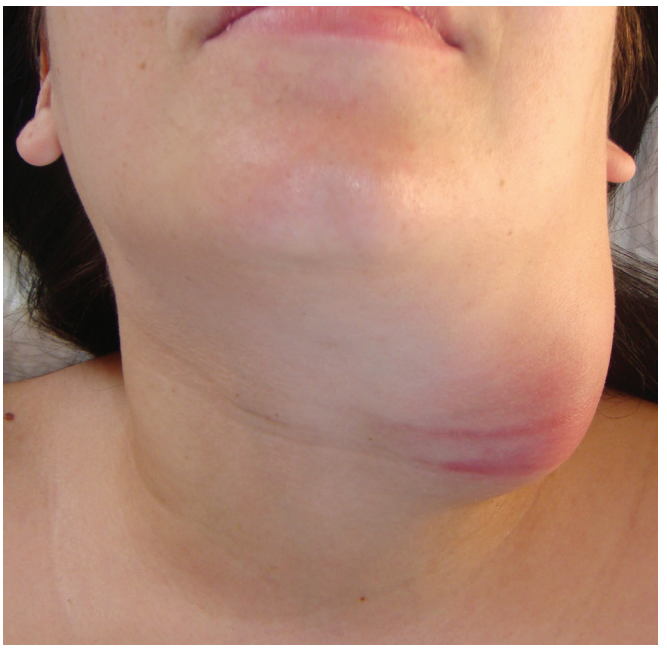

FIGURE 3. Clinical view of female with suppurated BCC.

cyst is a lymph node at the inferior pole. Upon swallowing the tumor-like mass does not move (as opposed to thyroglossal duct cysts). Consistency of the cysts are soft-elastic or elastically tense (elastically dense). A fluctuation may be determined. The BCCs does not cause respiratory and swallowing disorders. Systemic manifestations are not present. With secondary inflammation the cyst becomes dense, slow-moving, painful, can cause pain upon swallowing, and even talking. The systemic symptoms are (malaise, weakness, fever, etc.) appearing. Puncture of the cyst can get serous-mucous or muco-purulent transparent liquid light brown or dark brown (rare) color. Upon suppuration cyst fluid becomes turbid, pus appears. The skin over the cyst in case of its suppuration becomes hyperemated (Fig 3).

Desquamated epithelial cells, erythrocytes, lymphocytes, and cholesterol crystals can be detected microscopically in a punctate. Upon bacteriological examination a microflora in the content of uncomplicated cysts usually is not found. Only in rare cases low virulent *staphylococci* or *streptococci* are founded.

PATHOLOGY

Verification of the diagnosis is provided with pathomorphological investigation. Microscopically, the wall of the BCCs consists of a dense connective (fibrous) tissue that is lined with a stratified squamous non-cornified epithelium (ectodermal cysts), and multi-layered columnar epithelium (endodermal cyst). Some BCCs contain ciliated epithelium. Inside the wall (capsule) the lymphoid tissue, often forms the follicles (germinal centers) (Fig 4) [17]. Significant development of lymphoid tissue suggests that the BCCs originate from the branchial apparatus remnants. The inner surface of the cyst may be covered with warty growths of lymphoid tissue (crypts). In its wall, the formations like Hassel's corpuscles of thymus gland are identified. Upon suppuration of the cyst the epithelium can partially die and be replaced by the connective tissue, there is a thickening of the epithelial lining and its cornification. At the inferior pole of the BCCs the lymph node is often morphologically detected.

In front of the tragus, the preauricular (branchial) fistula can be found, which comes from I branchial pocket. The fistulous tract is lined by squamous epithelium. Preauricular (tragal) fistulas are often spread deep into the soft tissue to the parotid gland, and even penetrate into it. From these fistulas develop cysts localized in the parotid gland. The morphological difference between these fistulas is that the wall of the fistula, originating from the branchial I pocket has no lymphoid tissue, which is always present in BCCs or fistulas localized in the neck.

Diagnostics of BCCs is carried out between chronic **lymphadenitis** (non-specific and specific) [18-21], **dermoid** (**epidermoid**) **cysts** [22, 23], **tumors** and **tumor-like lesions** of soft tissues of the neck, blood vessels, nerves and thyroid gland, lymphangiomas (Fig 10) [24-28], metastases of malignant tumors, etc. For more accurate diagnosis the cyst- or fistulography with the administration of radiocontrast agents, CT, MRI, ultrasound can be performed (Fig 5).

ULTRASOUND

Upon **ultrasound diagnostics** are estimated: the location of the lesion, its size, wall thickness and the presence of septations, edges, borders, internal echogenicity, presence of acoustic enhancement artifact, fistula, vascularization at Doppler ultrasound. Compression of the mass by ultrasonic transducer confirms the true cystic nature helping in differential diagnosis. BCCs at ultrasonography are visualized as cystic mass of oval or round shape with smooth surface (Figs 6-8). Ahuja A.T. et al. (2000) [19] distinguish four echogenicity patterns of BCCs content: truly ***anehoic*** (41%), predominantly homogeneously ***hypoechoic*** but

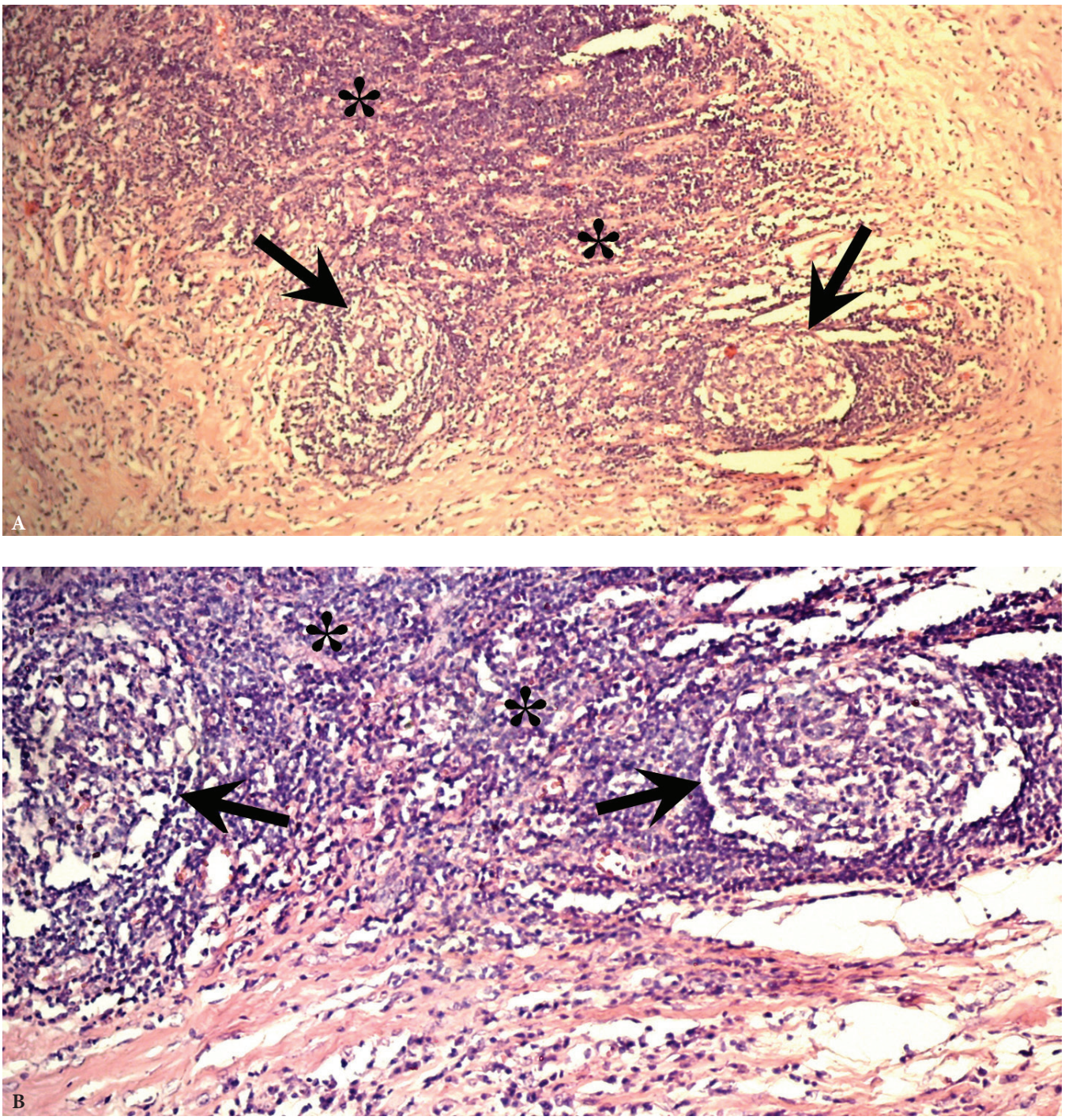

FIGURE 4. The histologic specimen of BCC of a 52-years-old female. Lymphoid formation (*asterisks*) in the thickness of the cystic wall with prominent bright breeding centers (germinal centers), which are marked by *arrows* (hematoxylin and eosin; magnification: **A** – x50, **B** – x100).

showing the presence of internal, low-amplitude, freely floating ***debris*** (diagnosed at 24%), ***hyperechoic*** with ***pseudosolid*** appearance (12%), ***heterogeneous*** internal echoes with internal debris and septa (23%). Echogenicity type is affected by the consistency of the content of the BCCs, which may vary depending on the presence of inflammatory processes (liquid-cystic, cystic-liquid with debris, pasty, suppurated). Pseudosolid appearance due to the presence of the protein content of the cysts produced by the epithelial lining [31]. On color and power Doppler ultrasound BCCs are avascular. Cyst wall appears as hyper- or isoehoic linear structure, often avascular at Doppler ultrasound. The thickness of the wall may vary in different parts of cysts and reach 1.0cm in recurrent inflammations [30,31], but also thinning is possible, i.e. the wall becomes non-differentiable [4].

CT & MRI

According to Weerakkody Y., Gaillard F. et al. on the **CT** and **MRI** images the BCCs have the following features.

For the patients with BCCs is recommended to perform magnetic resonance imaging in three modes. On **T1-weighted MR images** BCCs appears as a variable signal depending on the protein content. If their content is high – as high-intensity signal, low – as low intensity. On **T2-weighted MR images** BCCs are usually of high intensity. On **contrast-enhanced T1-weighted**

MRI, in uncomplicated cases, the BCCs have no enhancement.

On **contrast-enhanced multidetector CT images** BCCs are spherical or round shape, its walls are clearly distinguished from the surrounding tissue. The wall thickness varies from 0.1 to 1.0 cm. The cystic wall may penetrate between internal and external carotid arteries, in the region above the bifurcation of the common carotid artery (scraps symptom or beak tail) [6]. The density of the contents of the cavities (depending on the type of content and the presence of inflammation) ranges from 10 to +27,8 (± 6,0) HU, wall density is up to +102,0 (± 8,0) HU. **Hounsfield units** (HU) is a units of measure indicating the absorption of the X-rays by various tissues of the body. Remember that mostly absorbs x-rays the tooth enamel (3000 HU) and cortical bone (from 850 to 2000 HU), less of all – the blood (20-70 HU) and muscle (10-70 HU), adipose tissue (from −40 to −100 HU).

BCCs should be differentiated with esophageal diverticula. Esophageal diverticula is presented as a round shape lesion, which is located in front of sternocleidomastoid muscle. The lesion is soft or pastry to the touch, collapses on palpation and transmits peristaltic waves during swallowing. With eating it is filled, and increases in size. The pain is intensified with filling of diverticula after eating. Swallowing can be painful, especially during exacerbation of the inflammatory process.

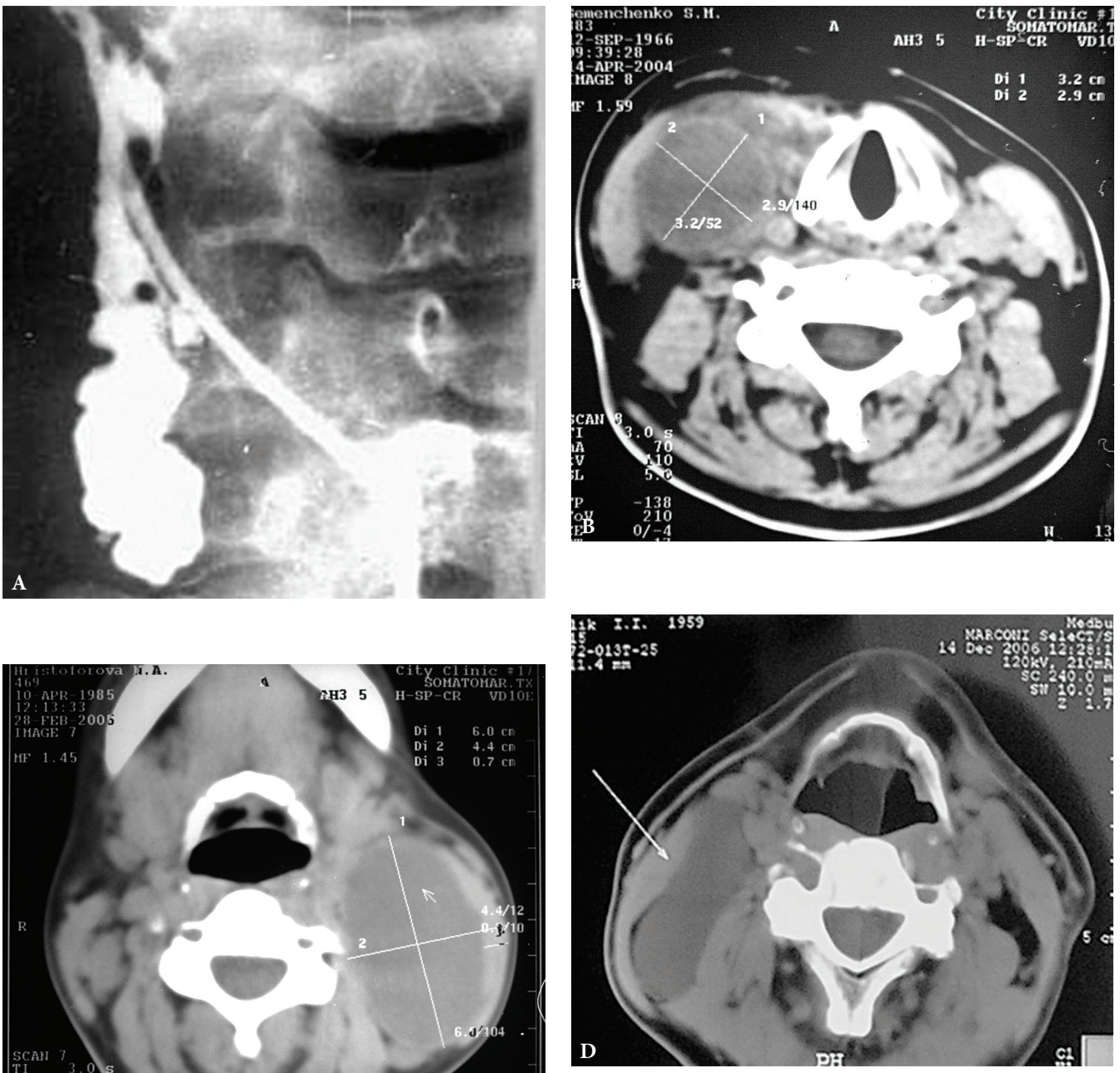

FIGURE 5. Cystogram (**A**) and CT images (**B**, **C**, **D**) of patients with BCCs.

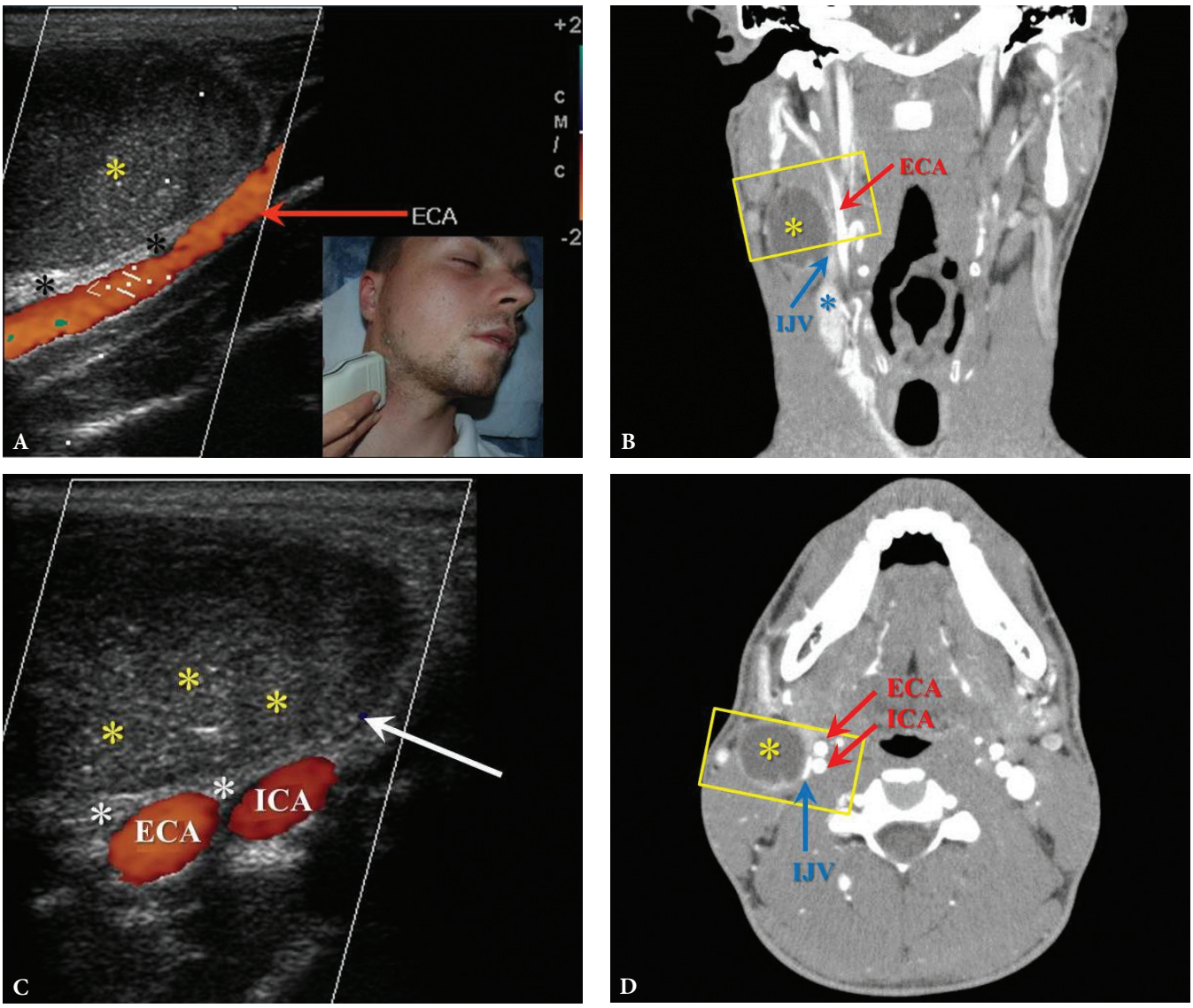

FIGURE 6. BCC in a 19-years-old patient. Longitudinal spectral Doppler sonogram (**A**) performed by linear transducer shows oval shaped cystic lesion with smooth margins, sharp edges, filled with a heterogeneous content (*yellow asterisks*) which simulate "pseudosolid" appearance. Note that cyst is adjacent to the external carotid artery (*ECA*) which is marked by a *red arrow*. Acoustic enhancement artifact (*black asterisks*) is distal to the cyst. Cyst is avascular. On contrast-enhanced CT (**B**) is confirmed the presence of cystic lesion (*yellow aterisk*) adjacent to the external carotid artery (*ECA*) and compression of the internal jugular vein (*IJV*). By *yellow frame* is marked the sonogram location performed at **Figure 6A**. Transverse spectral Doppler ultrasound (**C**) performed by linear transducer shows oval shaped cystic lesion with smooth contours, sharp edges, filled by heterogeneous content (*yellow asterisks*) which create "pseudosolid" appearance. The cyst is adjacent to the external (*ECA*) and internal carotid artery (*ICA*), and internal jugular vein (*IJV*), squeezing it (*white arrow*). Artifact of posterior acoustic enhancement (*white asterisks*) visualized distal to the cyst. Blood flow within the lesion and its wall is absent. On contrast CT image (**D**) confirmed the presence of cystic lesion (*yellow asterisk*) adjacent to the carotid arteries (*ECA, ICA*) and compression of the internal jugular vein (*IJV*). The density of the cyst content is +27,8 (± 6,0) HU. *Yellow frame* marks the position of a sonogram obtained at **Figure 6C**.

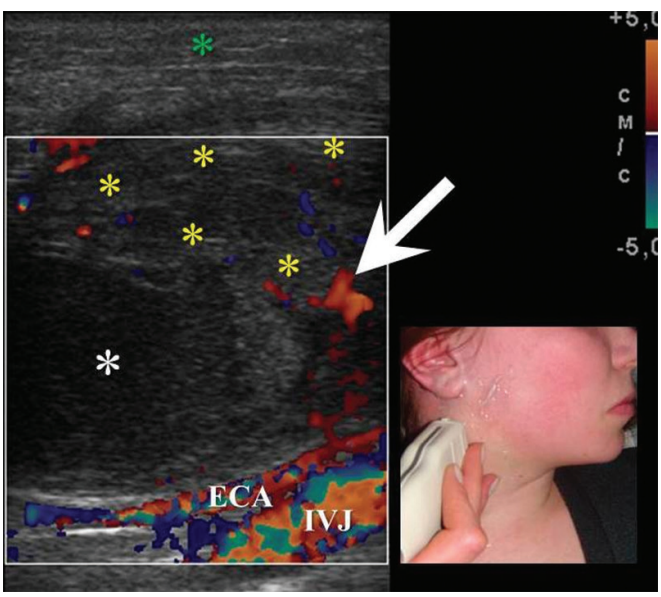

FIGURE 7. An infected BCC in a 18-years-old female. Longitudinal color Doppler ultrasound shows cystic oval shape lesion with hypoechoic content (*white asterisk*). Note inflammatory hyperemia of sternocleidomastoid muscle (*yellow asterisks*) in a form of its increased vascularity (*arrow*). Edema, decreased echogenicity of the surrounded tissues is marked by *green asterisk*. Lesion is avascular, adjacent to the neurovascular bundle of the neck. External carotid artery and internal jugular vein are marked by *ECA* and *IJV*.

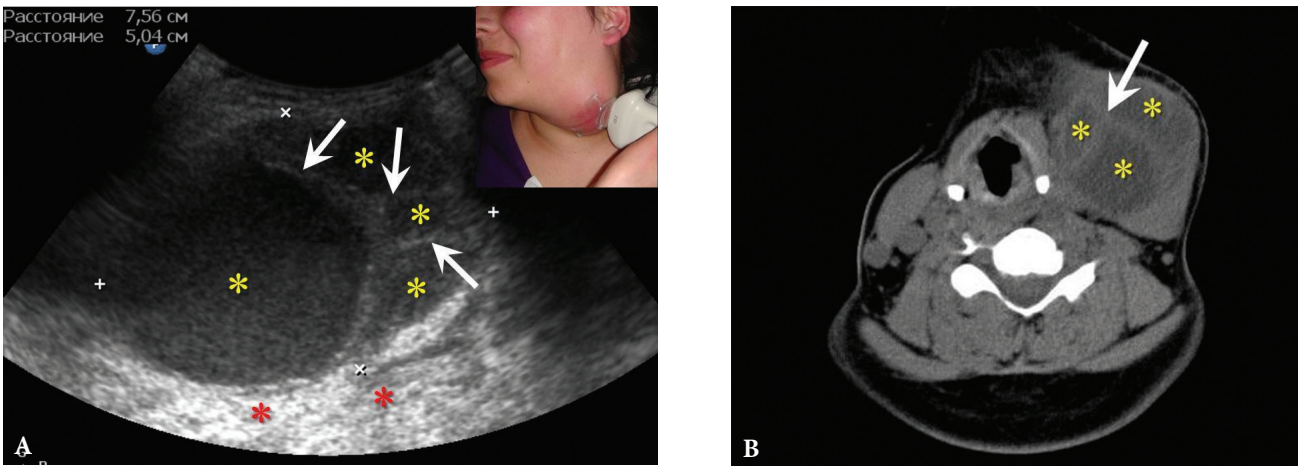

FIGURE 8. Suppurated multicameral BCC in a 33-years-old female. A sonogram (**A**) performed by convex transducer shows a cystic lesion (its size are marked with "+" and "x" are equal 7.5- x 5.0- cm) of the left neck with the presence of isoechoic septations (*arrows*). Anechoic cyst content in cameras are indicated by *yellow asterisks*, an artifact of acoustic enhancement – by *red asterisks*. An axial MDCT scan (**B**) confirms the presence of intracystic septations (*arrow*). The density of the cystic content is equal to +10, +15 HU. Cameras are marked by *asterisks*.

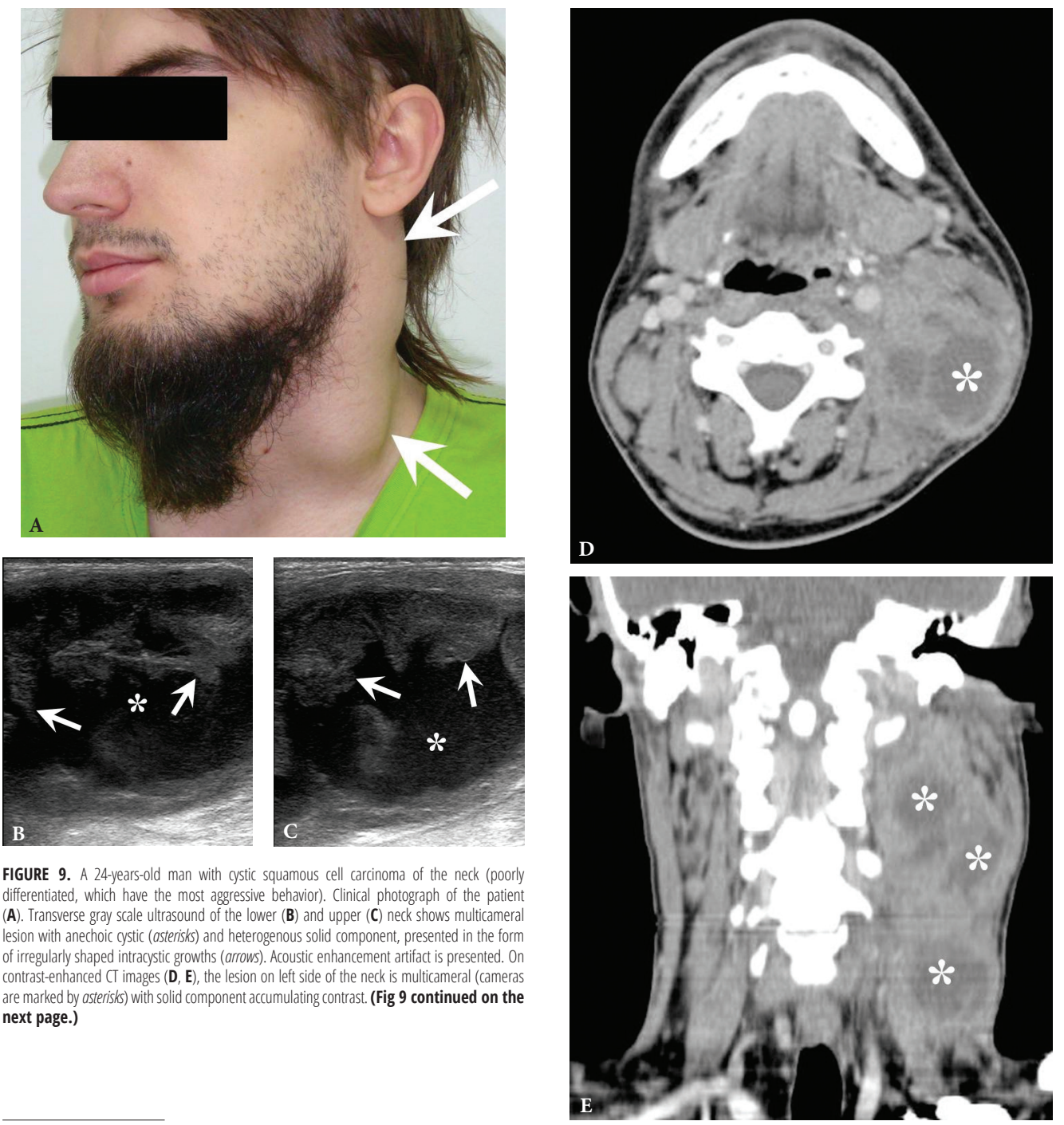

FIGURE 9. A 24-years-old man with cystic squamous cell carcinoma of the neck (poorly differentiated, which have the most aggressive behavior). Clinical photograph of the patient (**A**). Transverse gray scale ultrasound of the lower (**B**) and upper (**C**) neck shows multicameral lesion with anechoic cystic (*asterisks*) and heterogenous solid component, presented in the form of irregularly shaped intracystic growths (*arrows*). Acoustic enhancement artifact is presented. On contrast-enhanced CT images (**D**, **E**), the lesion on left side of the neck is multicameral (cameras are marked by *asterisks*) with solid component accumulating contrast. **(Fig 9 continued on the next page.)**

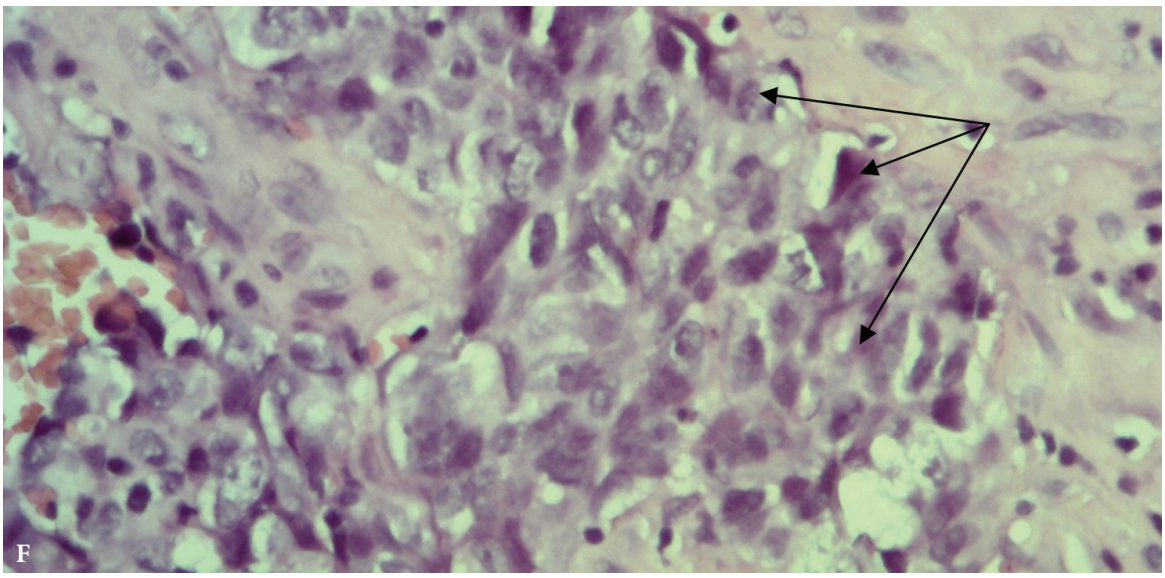

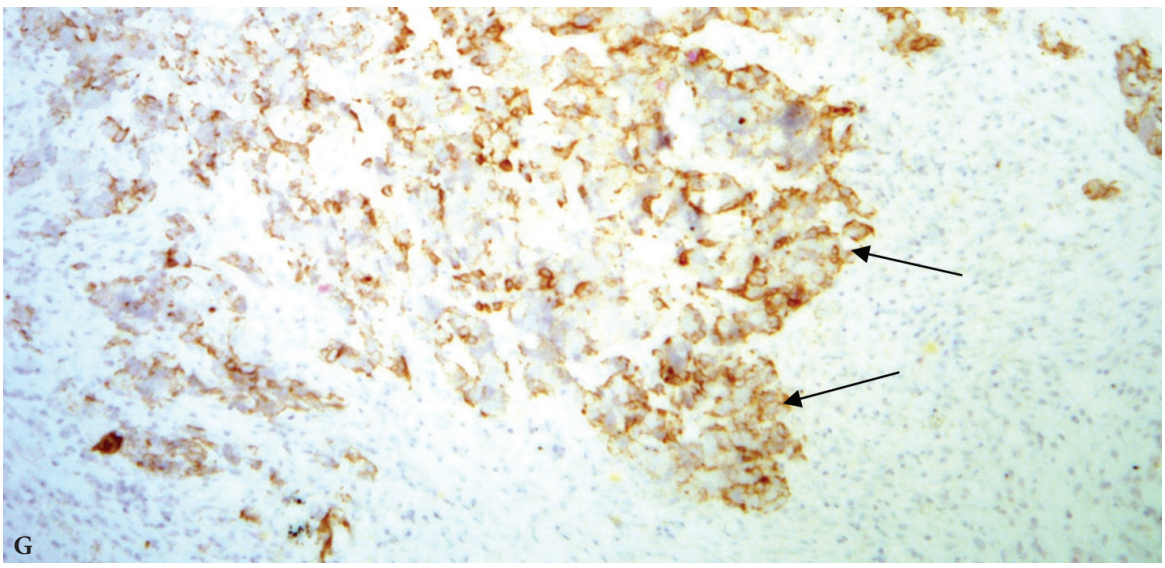

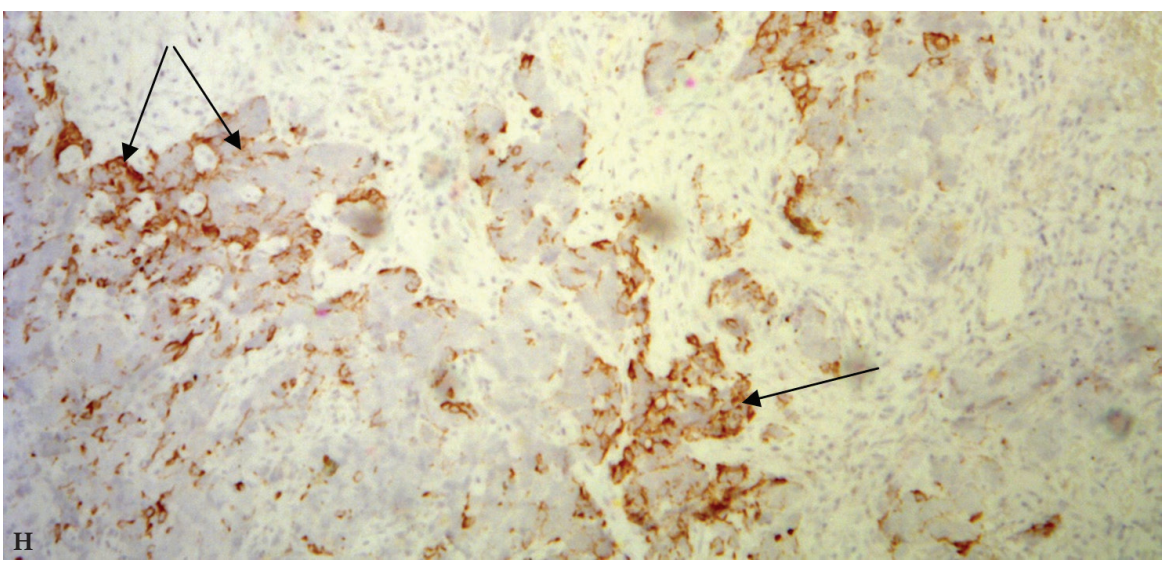

FIGURE 9 (cont'd). Trephine biopsy histology (**F**) shows, that in fragment of the lymph node tissue with presence of fibrous tissue, the growth of poorly differentiated malignant tumor (*arrows*) of epithelial nature with extensive necrosis in the tumor and lymph node tissue, hemorrhages is determined (hematoxylin and eosin; magnification x200). Immunohistochemistry (**G**, **H**) shows positive membrane reaction (*arrows*) with Cytokeratin AE1/AE3 and Cytokeratin 5/6. Reaction with CD45, S100 is negative (reaction with CD45- is determined in intact cells of the lymph node tissue). Thus, there is metastasis of poorly differentiated squamous cell carcinoma G_3 into lymphatic node tissue. (Histology and immunohistochemistry **Figure 9F**, **G**, **H** is courtesy of Dr. Antoniuk S.A., *Research Associate*, Dr. Petrenko L.I., *Junior Scientific Researcher*, Dr. Burtyn O.V., National Cancer Institute, Kyiv, Ukraine)

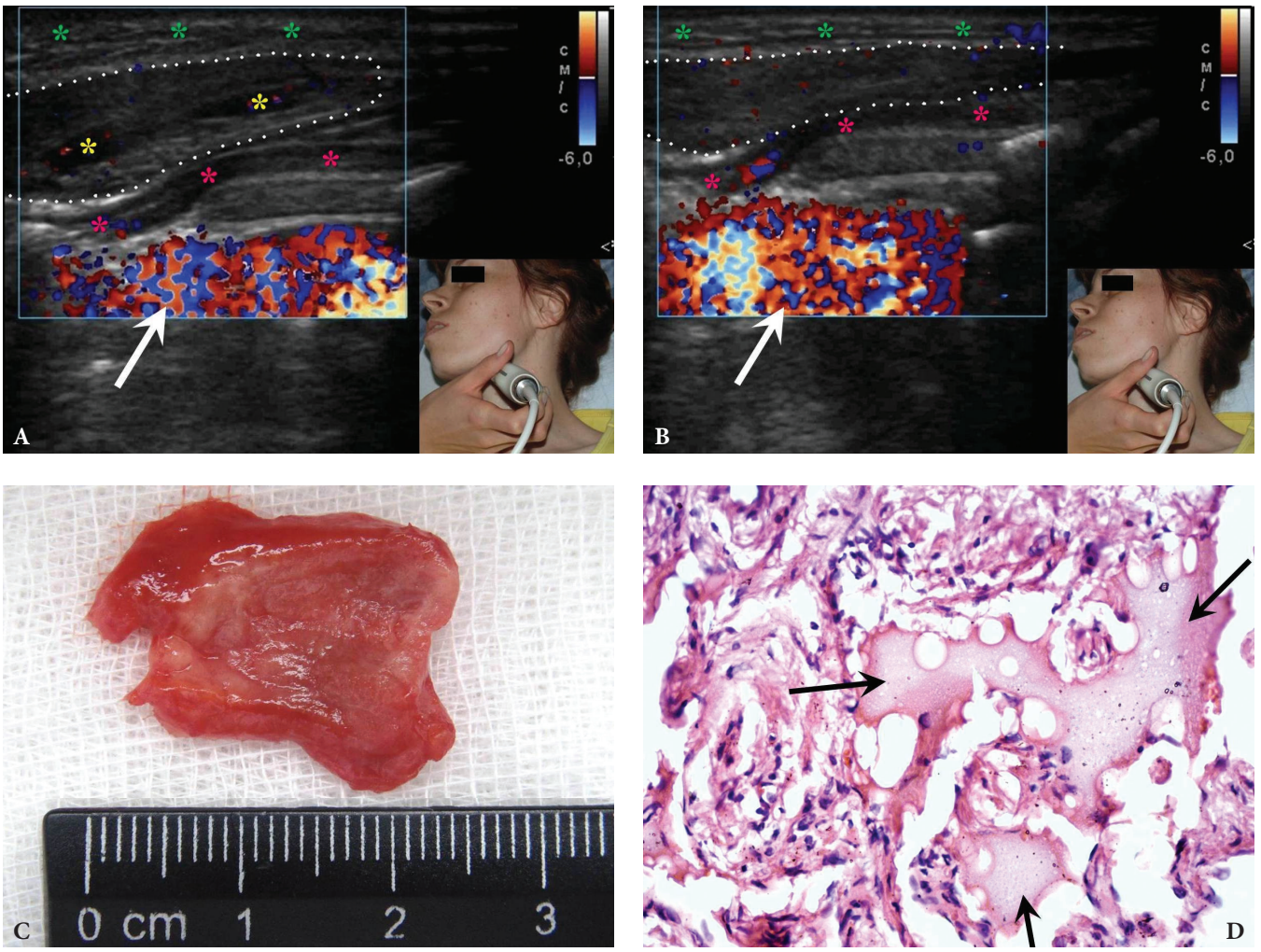

FIGURE 10. A 32-years-old female with cavernous lymphangioma of the upper neck. Oblique color Doppler ultrasound (**A**) shows well-demarcated lesion (marked by *white dots*) with a size of 3.0- × 1.0- cm elongated-oval form at the upper neck adjust to the omohyoid (*pink asterisks*) and anterior to the sternocleidomastoid muscles. Structure of the lesion is heterogeneous with presence of oval anechoic areas (cavities – *yellow asterisks*). The skin, subcutaneous tissue is marked by *green stars*. *White arrow* marks blooming artifact. Lesion have no arterial or venous blood flow. Oblique color Doppler ultrasound (**B**) with the compression by transducer (sonopalpation) noted the tumor shrinkage in 2-3 times, cavernous cameras are completely disappeared, indicating its spongy structure and confirmed after removal (lesion for the entire thickness was impregnated with light-gray liquid – lymph). Surgical specimen (**C**). Histology (**D**). In the lumen of the lymph vessels, lymph (*arrows*) is visualized. The inner layer is composed of endothelial cells of lymphatic vessels (oval form small inclusions with dark blue color). Hematoxylin and eosin; magnification x200.

TREATMENT

The treatment of the BCCs is only surgical (Figs 11, 12A). Surgery can be a difficult task due to the complex anatomical and topographical relations of the cysts with vessels and nerves of the neck. The surgery is performed under endotracheal anesthesia. The cut should be done on the anterior (medial) edge of the sternocleidomastoid muscle, or upper cervical crease. The first variant of incision is considered safer because in this area a large vessels and veins are located, and the second variant of cut is more cosmetic.

The surgeon may have difficulties in location place of internal pole of the BCC (Fig 1B), as in this place the internal jugular and facial veins are located. Especially need to be careful upon separating the BCC when its located nearby external and internal carotid arteries (Figs 12, 13). With the classical location of BCCs, it is more easy for the surgeon to navigate in the topographic anatomy of those vessels. However, often there are different variants for the location of the internal and external carotid arteries. This causes considerable difficulties in the intraoperative visualization of those vessels. Be especially careful in case of deep location of BCCs and the need to separate carotid arteries, i.e. topographic anatomy of the latter is not always classical (Fig 13).

COMPLICATIONS

Complications of BCCs the phlegmon of the and branchiogenic carcinoma are known. Phlegmon of the neck is more severe complication with severe intoxication in patient. Inflammatory processes can easily spread through the neurovascular bundle into the anterior mediastinum. Non-radical surgery may not only lead to recurrence, but also to the development of branchiogenic carcinoma (Figs 14, 15).

Branchiogenic carcinoma develops from the epithelium of the BCCs. Unlike cysts, tumor represents as a dense, tuberous, bad-movable (especially in the vertical direction) lesion, knitted with muscle and vascular bundle of the neck. Tumor (branchiogenic carcinoma) painless, relatively slow increases in size and can reach considerable size, quickly merges to the surrounding tissues. Tumor localization: from the submandibular region to the clavicle. Branchiogenic carcinoma merges to sternocleidomastoid muscle and vascular bundle of the

neck. If the tumor has not merge into the vascular bundle, it can be separated from the vessel. Malignant tumors can merge not only in vascular bundle neck, soft tissue (muscles) of the side of the neck, but to the pharynx and larynx. Histologically branchiogenic carcinoma usually has a structure of squamous cell carcinoma (Fig 9F, G, H).

Development of branchiogenic carcinoma, according to the Maxillofacial Surgery Department of Shupyk NMAPE, is about 4.5% of patients with BCCs. A high percentage of branchiogenic cancer in these patients emphasizes the need for early and proper performed surgery (removal of the BCC). Treatment of patients with branchiogenic carcinoma is combined. Prognosis is poor, often recurs, metastases are rare.

Branchiogenic carcinoma should be differentiated from the **carotid chemodectoma** (Fig 16) and other tumors of the neck. Carotid chemodectoma *synonyms: carotid body paraganglioma, glomus tumor, endothelioma, perithelioma, pheochromocytoma, paraganglioma, potato tumor, receptoma, etc.* Chemodectoma [34, 35] develops from the carotid sinus (*synonyms*: chemoreceptoral glomus, glomus caroticum), located at the adventitia layer inwards from the bifurcation of the common carotid artery.

Carotid sinus (Greek, *karóō* to put to sleep and sinus) is an expanded portion of the common carotid artery at the site of its branching into the external and internal arteries.

In this glomus there is a cluster of chromaffin cells around capillary glomeruli, and there is lot amount of nerve endings (functions as a "chemoreceptor" – responds to changes in the level of oxygen in the blood). Making pressure on the vessel in the area of carotid glomus leads to a slowing of heart rate. There carotid sinus baroreceptors are also located, when they are stimulated the blood vessels dilate and blood pressure falls. Chemodectomas are located under the sternocleidomastoid muscle at the point of common carotid artery bifurcation.

The skin over the tumor is not changed. Tumor has spherical or elongated form, with dimensions of 3.0cm or more, smooth or slightly tuberous. *A characteristic feature of chemodectoma is its horizontal displaceability and absence of displacement in vertical direction, the inability to move aside tumor from the pulsating vessel and "transfer pulsation" over the tumor.*

Macroscopically carotid chemodectoma has a light gray or brownish-red color and is surrounded by a connective tissue capsule (Fig 16C). Treatment of chemodectoma is surgical. Postoperative mortality is very high, i.e. in the vast majority it is not possible to separate the tumor from the common or internal carotid artery.

PROGNOSIS

With timely and correct performed surgery, removing of the BCCs, the prognosis is favorable.

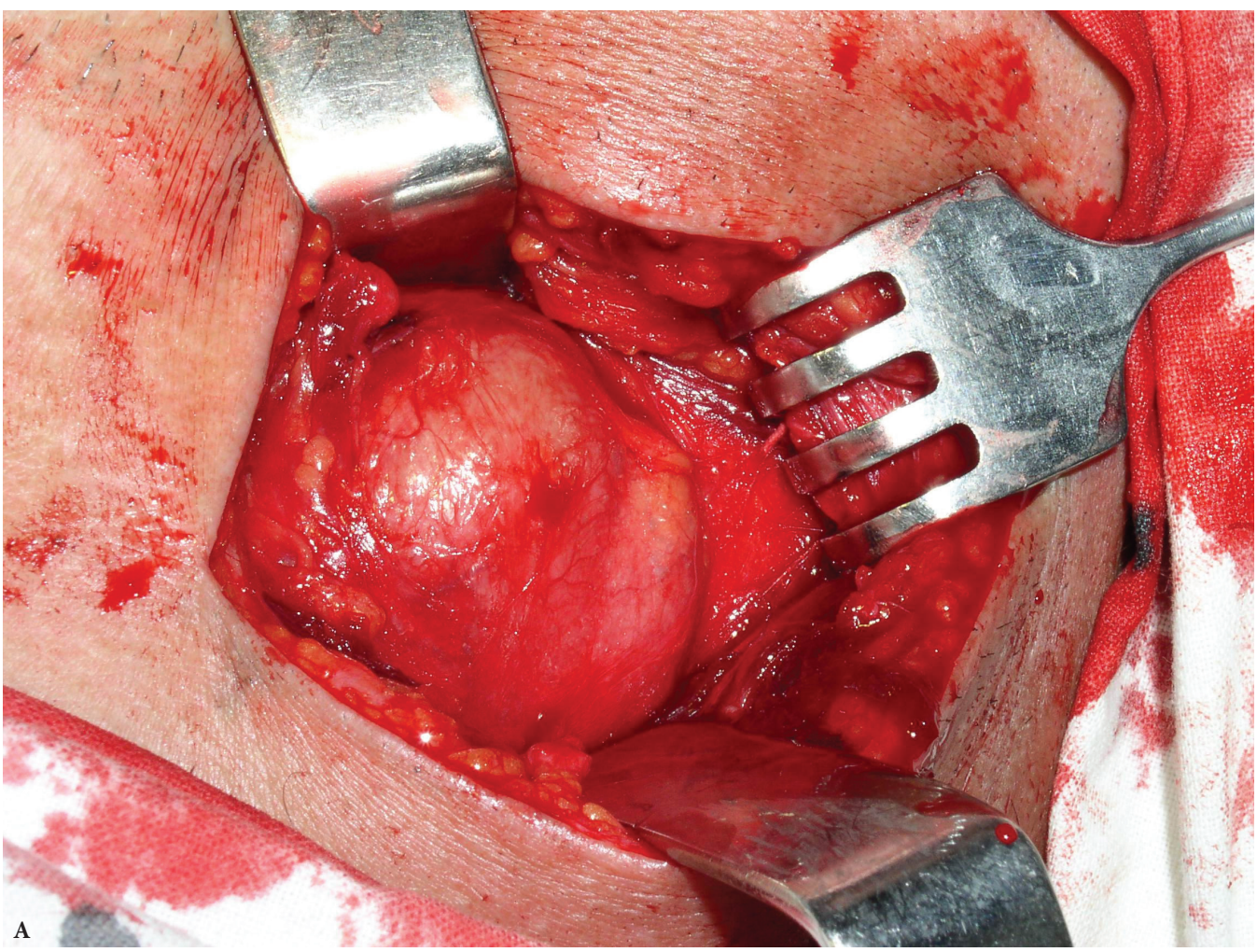

FIGURE 11. Surgical stage of BCC excision (**A**). **(Fig 11 continued on the next page.)**

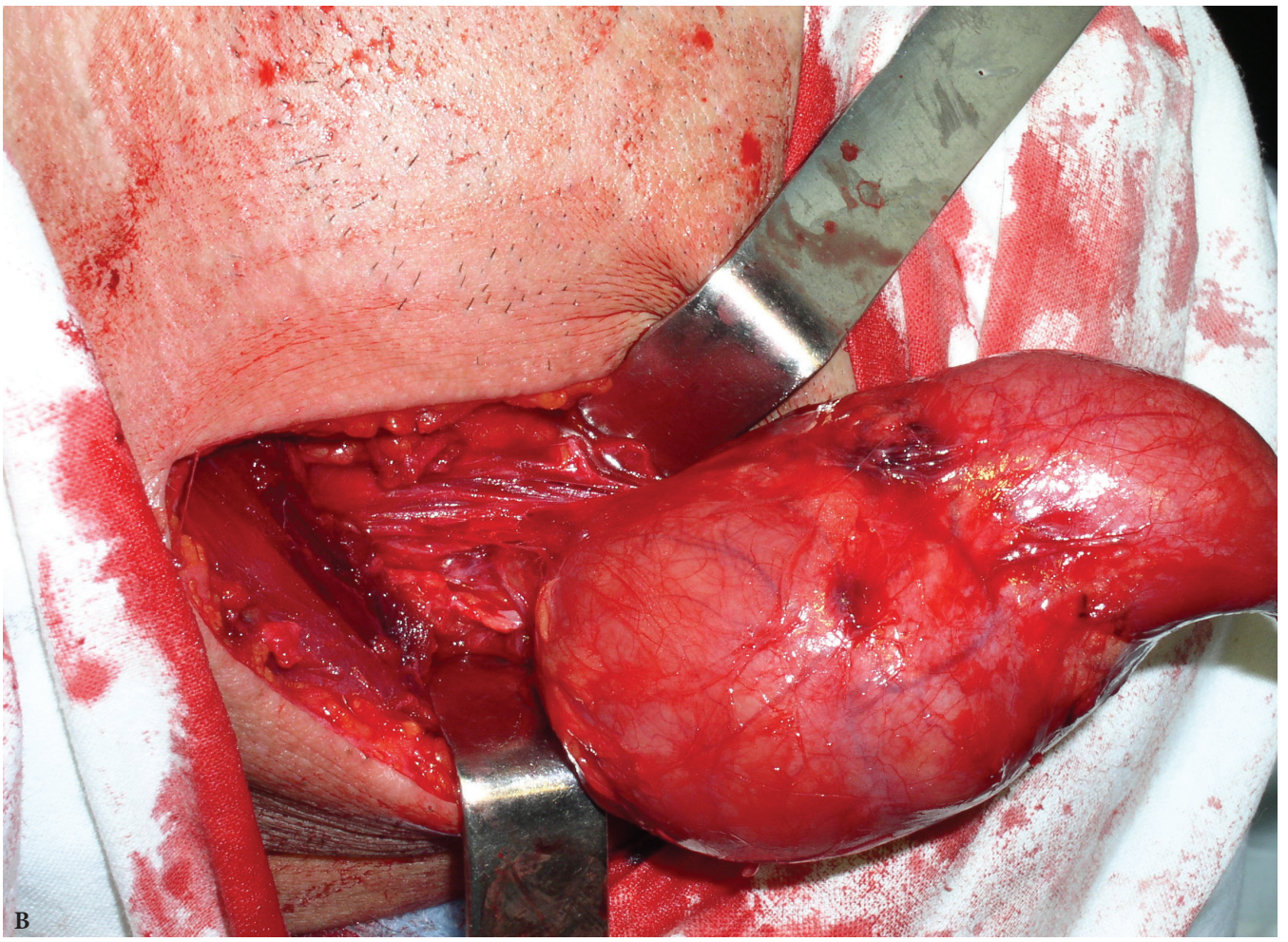

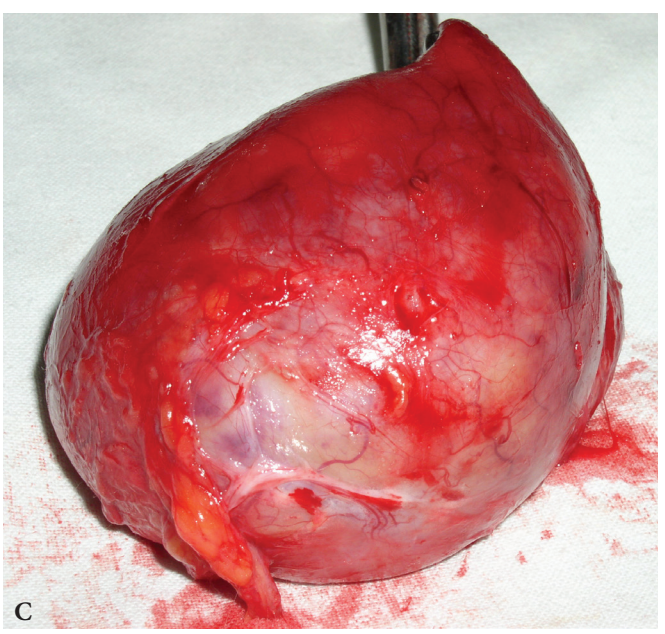

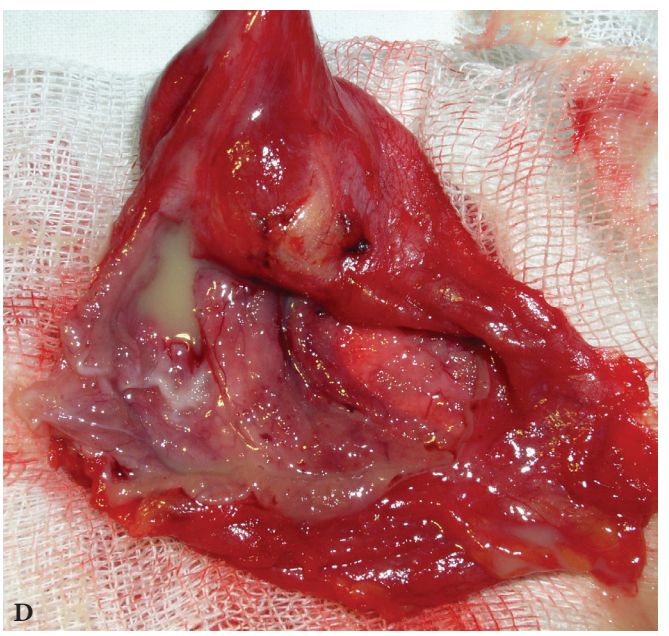

FIGURE 11 (cont'd). Surgical stage of BCC excision (**B**). View of BCC filled with content (**C**). View of the inner surface of cyst's wall (**D**) after its content evacuation.

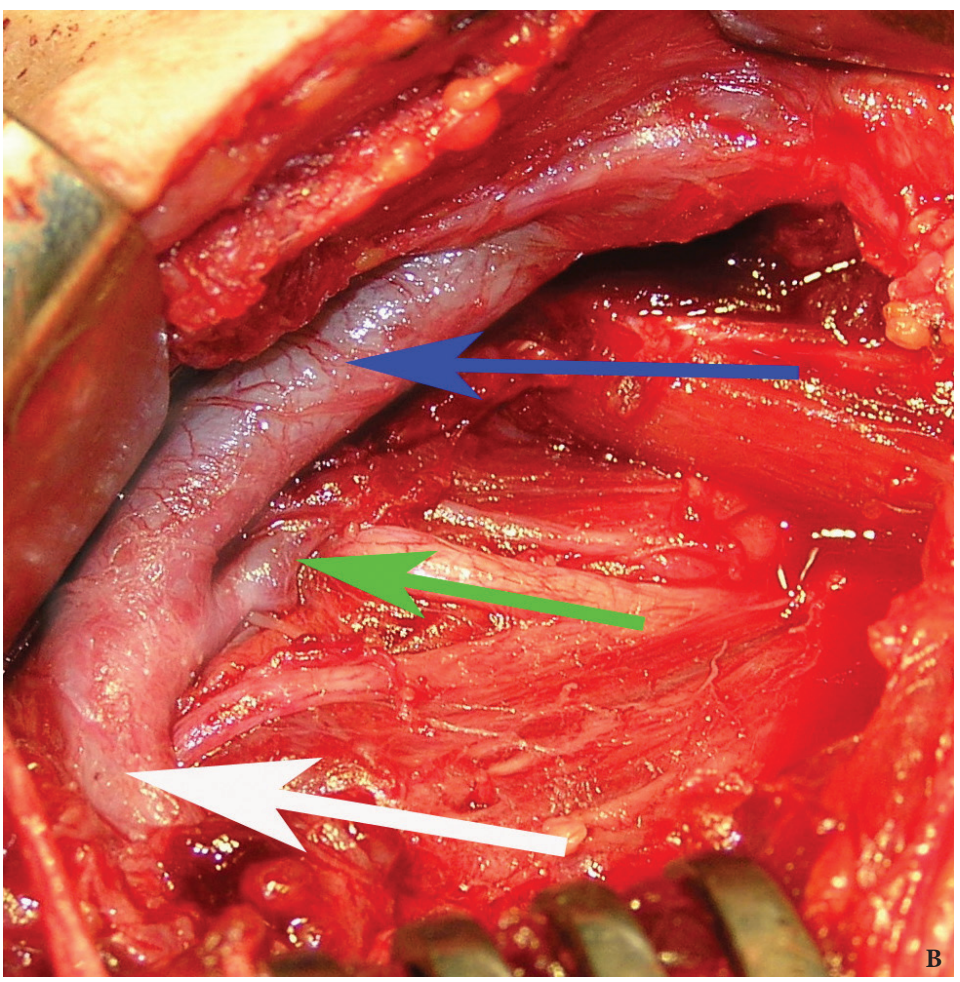

FIGURE 12. A stage of the BCC removing (**A**). *Black arrow* – BCC; *white arrow* – common carotid artery; *blue arrow* – external carotid artery; *green arrow* – internal carotid artery. View of the surgical wound after the BCC excision (**B**). *White arrow* – common carotid artery; *blue arrow* – external carotid artery; *green arrow* – internal carotid artery.

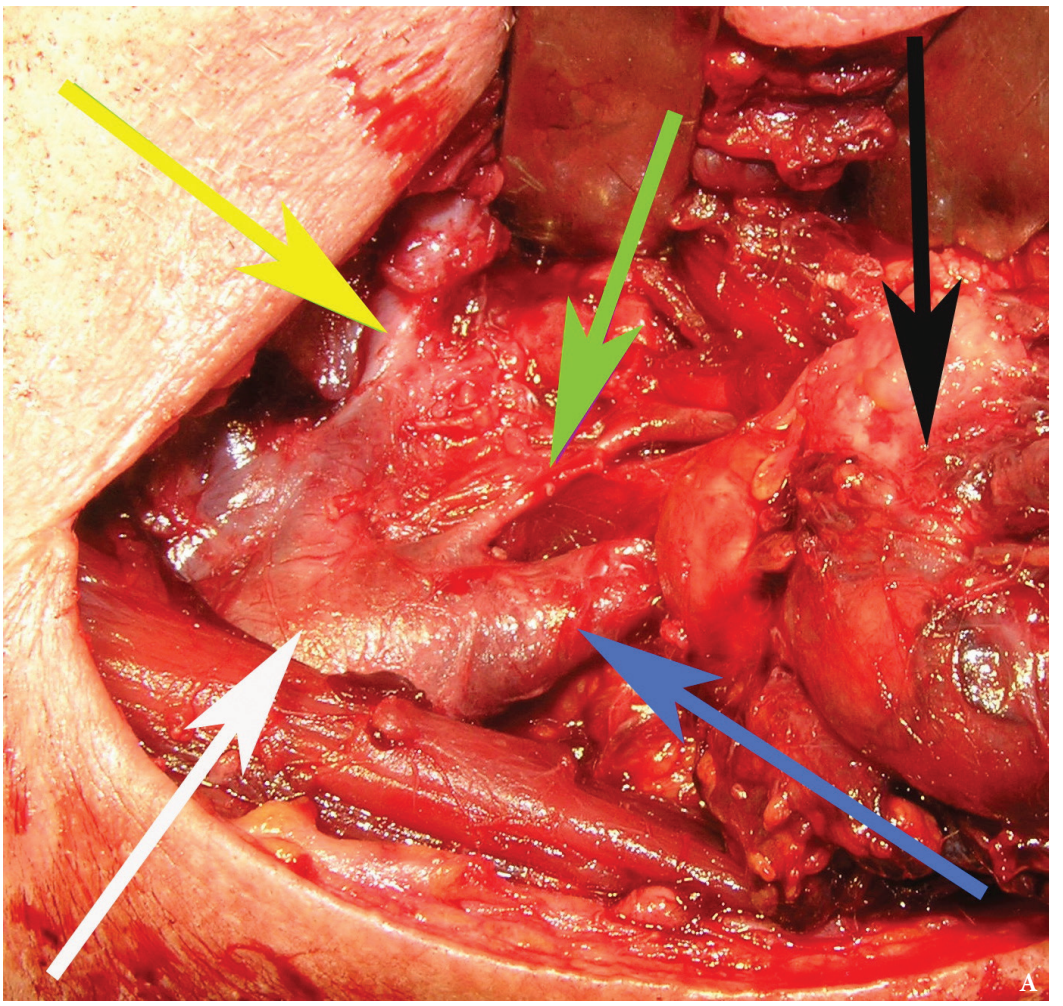

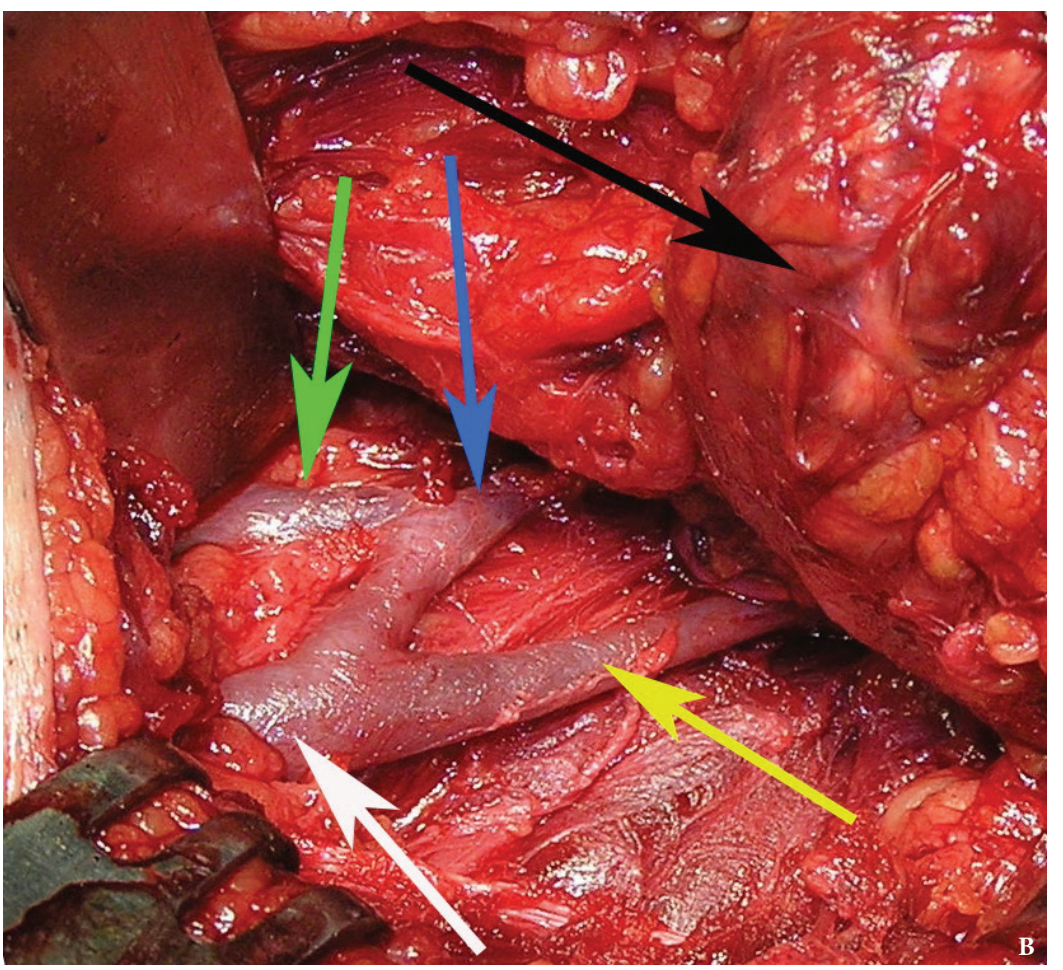

FIGURE 13. An intraoperative view of the surgical wound during the BCC removal (**A**, **B**). *Black arrow* – BCC; *white arrow* – common carotid artery; *yellow arrow* – internal carotid artery; *green arrow* – lingual artery; *blue arrow* – external carotid artery.

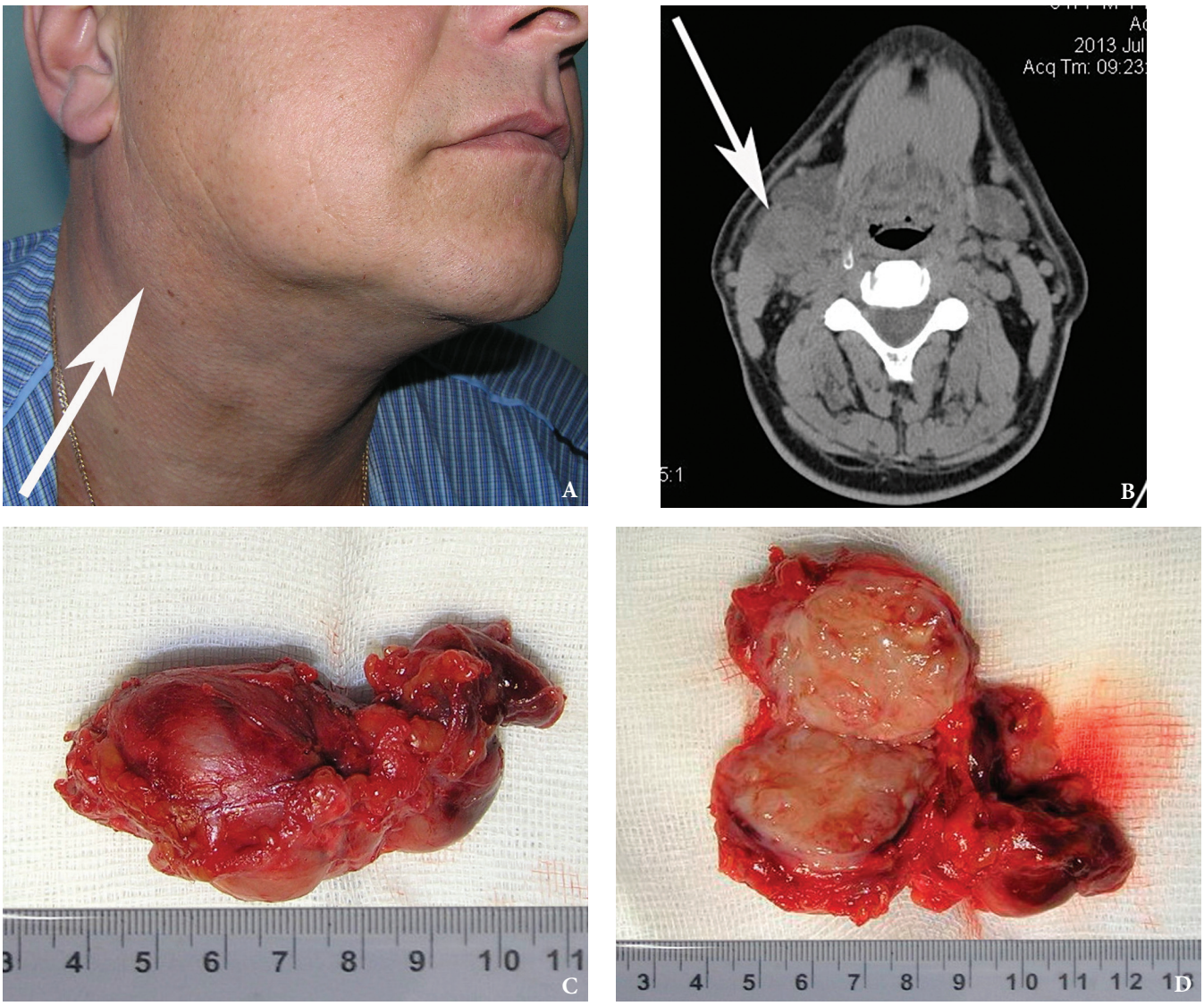

FIGURE 14. A patient with branchiogenic carcinoma (*arrow*) (**A**). Non-contrast CT image (**B**) shows the tumor (*arrow*). Tumor after its removal (**C**). Tumor on the section (**D**).

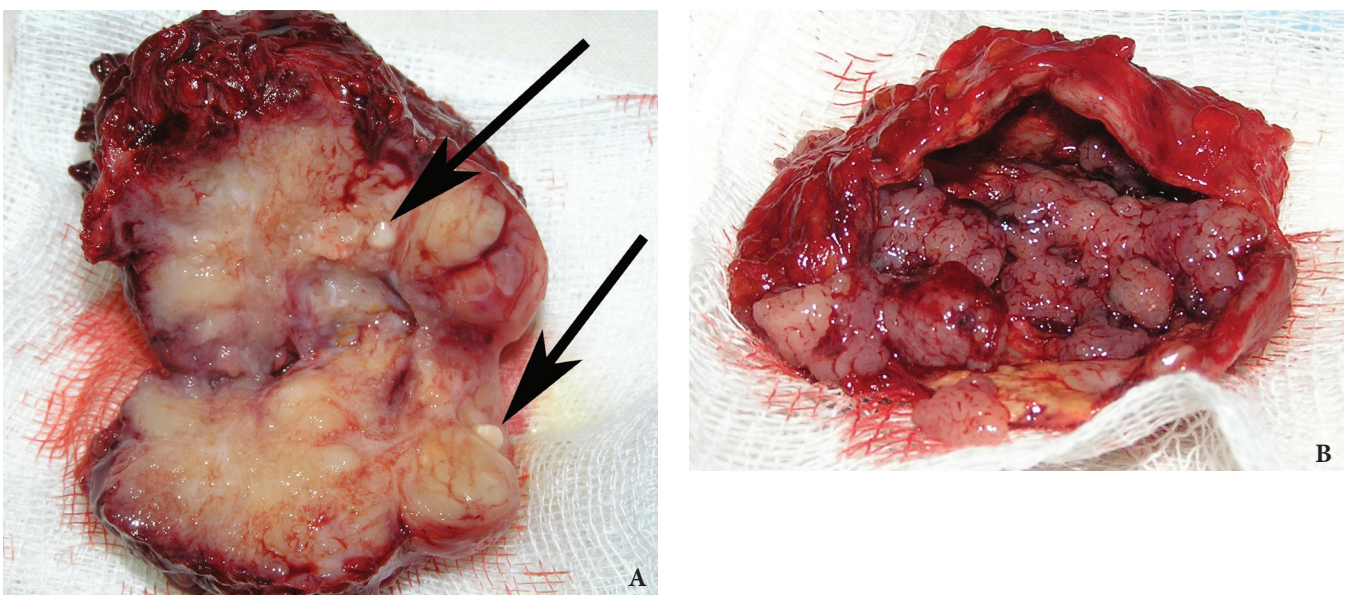

FIGURE 15. Macroscopic view of the branchiogenic carcinoma in different patients (**A**, **B**). Calcifications in malignant tumor are marked by *arrows* (**A**).

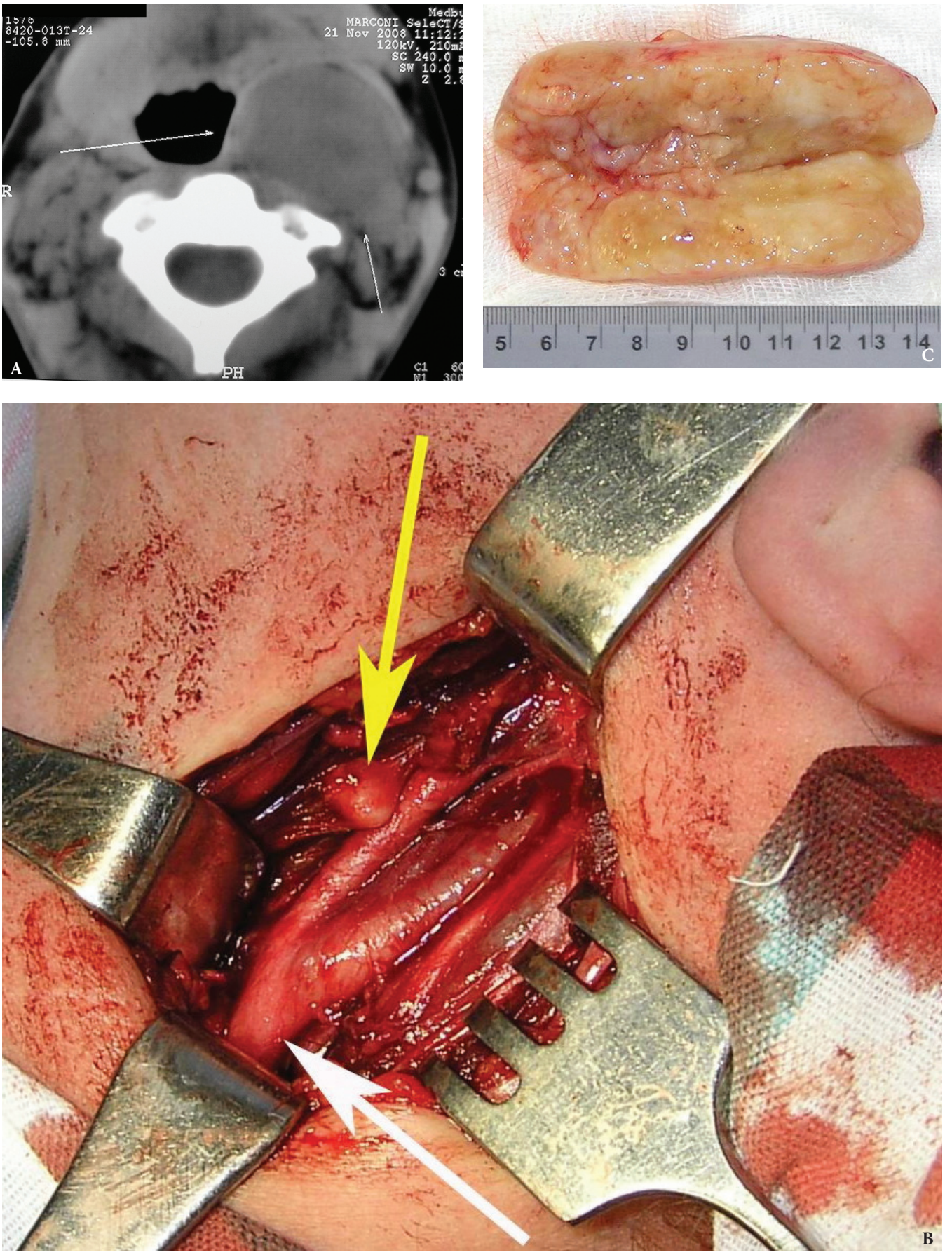

FIGURE 16. Computed tomography (**A**) of patient with carotid chemodectoma (*arrows*). Operating wound after chemodectoma removal (**B**). Common carotid artery – *white arrow*; greater horn of hyoid bone – *yellow arrow*. Macroscopic view of chemodectoma at section (**C**).

References

1. Tymofieiev AA. Rukovodstvo po chelustno-litsevoi hirurgii i hirurgicheskoi stomatologii [Manual of maxillofacial and oral surgery]. 5th ed. Kyiv: Chervona Ruta-Turs; 2012. p. 741−6 (in Russian).
2. Timofieiev AA. Chelustno-litsevaia hirurgiia [Maxillofacial surgery]. 2nd ed. Kyiv: Meditsina; 2015. p. 498−501 (in Russian).
3. Tymofieiev OO. Schelepno-lytseva hirurgiia [Maxillofacial surgery]. 1st ed. Kyiv: Meditsyna; 2011. p. 473−5 (in Ukrainian).
4. Kotliarov PM, Kharchenko VP, Aleksandrov YK, et al. Ultrazvukovaia diagnostika zabolevanii schitovidnoi zhelezy [Diagnostics ultrasound of the thyroid gland diseases]. 2nd ed. Vidar; 2009. p. 171, 172 (in Russian).
5. Lanham PD, Wushensky C. Second brachial cleft cyst mimic: case report. AJNR Am J Neuroradiol 2005;26:1862–4.
6. Chen PS, Lin YC, Lin YS. Nasopharyngeal branchial cleft cyst. Journal of the Chinese Medical Association 2012;75:660e662.
7. Chavan S, Deshmukh R, Karande P,et al. Branchial cleft cyst: A case report and review of literature. J Oral Maxillofac Pathol 2014;18:150.
8. Hu S, Hu CH, Yang L, et al. Atypical imaging observations of branchial cleft cysts. Oncol Lett 2014;7:219–22.
9. Bajaj Y, Tweedie D, Ifeacho S, et al. Surgical technique for excision of first branchial cleft anomalies: how we do it. Clin Otolaryngol 2011; 36:371–4.
10. Chan KC, Chao WC, Wu CM. Surgical management of first branchial cleft anomaly presenting as infected retroauricular mass using a microscopic dissection technique. Am J Otolaryngol 2012;33:20.
11. Guo YX, Guo CB. Relation between a first branchial cleft anomaly and the facial nerve. Br J Oral Maxillofac Surg 2012;50: 259–63.
12. Pradipta KP, Arun A, Kalairasi R, et al. First branchial cleft malformation with duplication of external auditory canal. Case Reports in Otolaryngology 2013;2013:1−5.
13. Krishnamurthy A, Ramshanker VA. Type I first branchial cleft cyst masquerading as a parotid tumor. Natl J Maxillofac Surg 2014;5:84–85.
14. Joshi MJ, Provenzano MJ, Smith RJ, et al. The rare third branchial cleft cyst. AJNR Am J Neuroradiol 2009;30:1804−6.
15. Adams A, Mankad K, Offiah C, et al. Branchial cleft anomalies: a pictorial review of embryological development and spectrum of imaging findings. Insights Imaging 2016;7:69–76.
16. Bailey H. Branchial cysts and other essays on surgical subjects in the faciocervical region. London: Lewis,1929.
17. Wenig BM. Atlas of head and neck pathology. 3rd ed. Elsevier; 2015. p. 538−46.
18. Mittal MK, Malik A, Sureka B, et al. Cystic masses of neck: a pictorial review. Indian J Radiol Imaging 2012;22:334−43.
19. Ahuja A, Ying M. Sonographic evaluation of cervical lymphadenopathy: is power Doppler sonography routinely indicated? Ultrasound Med Biol 2003;29:353–9.
20. Zenk J, Bozzato A, Steinhart H, et al. Metastatic and inflammatory cervical lymph nodes as analyzed by contrast-enhanced color-coded Doppler ultrasonography: quantitative dynamic perfusion patterns and histopathologic correlation. Ann Otol Rhinol Laryngol 2005;114:43–7.
21. Hsieh YY, Hsueh S, Hsueh Ch, et al. Pathological Analysis of Congenital Cervical Cysts in Children: 20 Years of Experience at Chang Gung Memorial Hospital. Chang Gung Med J 2003;26:107−13.
22. Pryor SG, Lewis JE, Weaver AL, et al. Pediatric dermoid cysts of the head and neck. Otolaryngol Head Neck Surg 2005;132:938−42.
23. Dutta M, Saha J, Biswas G, et al. Epidermoid Cysts in Head and Neck: Our Experiences, with Review of Literature. Indian J Otolaryngol Head Neck Surg 2013;65(Suppl 1):14–21.
24. Amer I, Choudhury N, Falzon A, et al. Cystic neck masses – a diagnostic and management challenge. SAJ Cas Rep 2014;1:1−4.
25. Kraus J, Plzák J, Bruschini R, et al. Cystic lymphangioma of the neck in adults: a report of three cases. Wien Klin Wochenschr. 2008;120:242−5.
26. Karkos PD, Spencer MG, Lee M, et al. Cervical cystic hygroma/lymphangioma: an acquired idiopathic late presentation. J Laryngol Otol 2005;119:561–3.
27. Kennedy TL, Whitaker M, Pellitteri P, et al. Cystic hygroma/lymphangioma: a rational approach to management. Laryngoscope 2001;111:1929–37.
28. Grasso DL, Pelizzo G, Zocconi E, et al. Lymphangiomas of head and neck in children Acta Otorhinolaryngol Ital 2008;28:17–20.
29. Dutta M, Kundu S, Ghosh B. Cystic squamous cell carcinoma of the neck: could a second metastatic focus help? Otolaryngologia Polska 2014;68:338−41.
30. Ahuja AT, King AD, Metreweli C. Second branchial cleft cysts: variability of sonographic appearances in adult cases. AJNR Am J Neuroradiol 2010;21:315–9.
31. Yuen HY, Ahuja AT. Chapter 11: benign clinical conditions in the adjacent neck. In: Sofferman RA, Ahuja AT, editors. Ultrasound of the thyroid and parathyroid glands. Springer; 2012. p. 229−33.
32. Caly DN, Viana A, Rapoport A, et al. Indications and pitfalls of immunohistochemistry in head and neck cancer. Braz J Otorhinolaryngol 2013;79:75−81.
33. Naswa N, Kumar A, Sharma P, et al. Imaging carotid body chemodectomas with 68Ga-DOTA-NOC PET-CT. Br J Radiol 2012;85(1016):1140–5.
34. Davidovic LB, Djukic VB, Vasic DM, et al. Diagnosis and treatment of carotid body paraganglioma: 21 years of experience at a clinical center of Serbia. World J Surg Oncol 2005; 3:10.
35. Durdik S, Malinovsky P. Chemodectoma − carotid body tumor surgical treatment. Bratisl Lek Listy 2002;103:422−3.

Tymofieiev OO, Fesenko IeI, Cherniak OS, Zaritska VI.
Features of diagnostics, clinical course and treatment of the branchial cleft cysts.
J Diagn Treat Oral Maxillofac Pathol 2017;1:15−31.

Особливості діагностики, клінічного перебігу і лікування бранхіогенних кіст шиї

Олексій О. Тимофєєв[1], Євген І. Фесенко[2], Ольга С. Черняк[3], Валентина І. Заріцька[4]

[1] Завідувач кафедри щелепно-лицевої хірургії Інституту стоматології Національної медичної академії післядипломної освіти імені П.Л. Шупика, д.мед.н., професор, Заслужений діяч науки і техніки України, Київ, Україна.
[2] Асистент кафедри хірургічної стоматології та щелепно-лицевої хірургії КМУ УАНМ, Київ, Україна.
[3] Завідувач відділенням ультразвукової діагностики Обласного діагностичного центру Київської обласної клінічної лікарні, Київ, Україна.
[4] Доцент кафедри патологічної і топографічної анатомії НМАПО імені П.Л. Шупика, к.мед.н., Київ, Україна.

ПРО СТАТТЮ

Історія рукопису:

Отриманий: 03 жовтня 2016
Прийнятий: 08 листопада 2016
Онлайн з: 18 лютого 2017

Ключові слова:

Бранхіогенна кіста шиї
Бранхіогенний рак
МСКТ
Одиниці Хаунсфілда
МРТ
УЗД
Ехогенність
Колірне допплерівське картування
Псевдосолідність

РЕЗЮМЕ

Мета. Визначити особливості діагностики, клінічного перебігу та лікування бранхіогенних кіст шиї.
Методи. Бранхіогенні кісти шиї та їх ускладнення у пацієнтів різних вікових груп, методи їх діагностики, анатомічні особливості, етапи операції і патоморфологічне дослідження.
Результати. Доведено діагностичну цінність ехографії, МСКТ і МРТ, патоморфологічного дослідження у верифікації бранхіогенних кіст шиї та їх ускладнень. Описано методику проведення оперативних втручань.
Висновки. Описані нами методи діагностики бранхіогенних кіст шиї та їх ускладнень, варіанти клінічного перебігу та методи лікування дозволяють знизити ризик помилок на до-, інтра- і післяопераційному етапах.

Особенности диагностики, клинического течения и лечения бранхиогенных кист шеи

Алексей А. Тимофеев[1], Евгений И. Фесенко[2], Ольга С. Черняк[3], Валентина И. Зарицкая[4]

[1] Заведующий кафедрой челюстно-лицевой хирургии Института стоматологии Национальной медицинской академии последипломного образования имени П.Л. Шупика, д.мед.н., профессор, Заслуженный деятель науки и техники Украины, Киев, Украина.
[2] Ассистент кафедры хирургической стоматологии и челюстно-лицевой хирургии КМУ УАНМ, Киев, Украина.
[3] Заведующая отделением ультразвуковой диагностики Областного диагностического центра Киевской областной клинической больницы, Киев, Украина.
[4] Доцент кафедры патологической и топографической анатомии НМАПО имени П.Л. Шупика, к.мед.н., Киев, Украина.

О СТАТЬЕ

История рукописи:

Получена: 03 октября 2016
Принята: 08 ноября 2016
Онлайн с: 18 февраля 2017

Ключевые слова:

Бранхиогенная киста шеи
Бранхиогенный рак
МСКТ
Единицы Хаунсфилда
МРТ
УЗД
Эхогенность
Цветовое допплеровское картирование
Псевдосолидность

РЕЗЮМЕ

Цель. Определить особенности диагностики, клинического течения и лечения бранхиогенных кист шеи.
Методы. Бранхиогенные кисты шеи и их осложнения у пациентов разных возрастных групп, методы их диагностики, анатомические особенности, этапы операции и патоморфологическое исследование.
Результаты. Доказано диагностическую ценность эхографии, МСКТ и МРТ, патоморфологического исследования в верификации бранхиогенных кист шеи и их осложнений. Описано методику проведения оперативных вмешательств.
Выводы. Описанные нами методы диагностики бранхиогенных кист шеи и их осложнений, варианты клинического течения и методы лечения позволяют снизить риск ошибок на до-, интра- и послеоперационном этапах.